HIGH CURRENT COAXIAL PULSE TRANSFORMER FOR RAILGUN APPLICATIONS

J. A. Pappas
U. S. Army Armament Research and Development Center
EM Launch Research
Dover, NJ 07801

M. D. Driga and W. F. Weldon
Center for Electromechanics
The University of Texas at Austin
Austin, TX 78712

Summary

A high-current air-core pulse transformer has been designed and fabricated. Its purpose is to reduce the output impedance (nominally 100 mΩ) of a 50-kJ, 1,000-μF capacitor bank for application to loads with impedances of about 25 mΩ. The system will be used for high current component testing, specifically experimental evaluation of the pressure limits of high-strength wrapped hypervelocity railgun sections.

The transformer will be part of a test stand consisting of five capacitor bank/transformer sets capable of delivering up to 1.5 million A to a load. The geometry of the transformer is coaxial. The secondary coil consists of circular aluminum tubes connected in parallel. The primary winding is contained within the tubes and is connected in series. The coaxial geometry was chosen for its high coupling coefficient and its mechanical simplicity. Design improvements and future refinements are also discussed.

Introduction

The electromagnetic launch facility at Picatinny Arsenal has five modular energy discharge capacitor banks, each with a storage capacity of 50 kJ, operating at 10 kV, and capable of producing 100-kA peak current.

It was desired to use these banks as the prime energy stores for a high magnetic pressure test stand. The purpose of this fixture is to test various materials as part of the design of the AGATE high pressure railgun system currently being developed.

In order to achieve the high currents (> 1 MA) necessary to obtain barrel design pressure of 1,13.47 MPa, the rated bank current of 100 kA must be increased. An air-core coaxial pulse transformer is an attractive candidate for matching the high output impedance of the capacitor bank to the railgun input. Among the benefits of the coaxial geometry are the high coupling coefficient, low external field, simple electromagnetic modeling, compactness, and easy fabrication.

A related application for a pulse transformer has been proposed allowing the high current levels required by mass accelerators from low current generators.[1] This would ease the design problems associated with current collection through sliding contacts. However, the proposed design does not assure tight coupling between the secondary and primary, which finally would affect the overall performance.

The degree of coupling for different types of pulse transformers is analyzed by Sadedin. Various geometries are considered such as a separate layer winding, a bifilar winding, a thin sheet, and a coaxial cable. The analysis shows that the coaxial cable type is by far the most effective in terms of high coefficient of coupling.[2]

The pulse transformer can perform more complex and subtler roles; e.g., a fast power crowbar system for fast theta-pinch experiments and the success of the experiments depends on attaining extremely low values for the leakage inductance.[3] But also, it acts as a transient energy storage and as an element in a special type of flux compression in order to produce the plasma initiation pulse for ohmic heating in a thermonuclear fusion reactor.[4]

Theoretical

The engineering perception about transformers is biased by the long experience with operation of such devices in sinusoidal (harmonic) regime. Equivalent circuits obtained through phasor methods do not apply to the transformers acting in pulsed regime and the operational method must be used to find the response of the circuit to a unit step-function. Given response to the unit step-function, using the convolution theorem one can find the response for any type of input. For the idealized transformer (fig. 1) the equations written using Laplace transform are

$$sL_1I_1(s) + sMI_2(s) + R_1I_1(s) = \frac{1}{s}$$

$$sL_2I_2(s) + sMI_1(s) + R_2I_2(s) = 0 \quad .$$

Solving for currents,

$$I_1(s) = \frac{sL_2 + R_2}{(L_1L_2 - M^2)s^2 + (R_1L_2 + R_2L_1)s + R_1R_2}$$

$$I_2(s) = \frac{-sM}{(L_1L_2 - M^2)s^2 + (R_1L_2 + R_2L_1)s + R_1R_2}$$

$$I_1(s) = \frac{1}{L_1L_2 + M^2} \cdot \frac{sL_2 + R_2}{s^2 + 2\alpha s + \omega_o^2}$$

$$I_2(s) = \frac{-1}{L_1L_2 + M^2} \cdot \frac{sM}{s^2 + 2\alpha s + \omega_o^2}$$

where,

$$\alpha = \frac{R_1L_2 + R_2L_1}{2(L_1L_2 - M^2)} \ , \quad \omega_o^2 = \frac{R_1R_2}{(L_1L_2 - M^2)} \ ,$$

$$\text{and } \omega = \sqrt{\alpha^2 - \omega_o^2} \quad .$$

Report Documentation Page

Form Approved
OMB No. 0704-0188

1. REPORT DATE **JUN 1985**	2. REPORT TYPE **N/A**	3. DATES COVERED **-**

4. TITLE AND SUBTITLE **High Current Coaxial Pulse Transformer For Railgun Applications**	5a. CONTRACT NUMBER
	5b. GRANT NUMBER
	5c. PROGRAM ELEMENT NUMBER
6. AUTHOR(S)	5d. PROJECT NUMBER
	5e. TASK NUMBER
	5f. WORK UNIT NUMBER
7. PERFORMING ORGANIZATION NAME(S) AND ADDRESS(ES) **U. S. Army Armament Research and Development Center EM Launch Research Dover, NJ 07801**	8. PERFORMING ORGANIZATION REPORT NUMBER
9. SPONSORING/MONITORING AGENCY NAME(S) AND ADDRESS(ES)	10. SPONSOR/MONITOR'S ACRONYM(S)
	11. SPONSOR/MONITOR'S REPORT NUMBER(S)

12. DISTRIBUTION/AVAILABILITY STATEMENT
Approved for public release, distribution unlimited

13. SUPPLEMENTARY NOTES
See also ADM002371. 2013 IEEE Pulsed Power Conference, Digest of Technical Papers 1976-2013, and Abstracts of the 2013 IEEE International Conference on Plasma Science. Held in San Francisco, CA on 16-21 June 2013. U.S. Government or Federal Purpose Rights License

14. ABSTRACT

15. SUBJECT TERMS

16. SECURITY CLASSIFICATION OF:			17. LIMITATION OF ABSTRACT	18. NUMBER OF PAGES	19a. NAME OF RESPONSIBLE PERSON
a REPORT **unclassified**	b ABSTRACT **unclassified**	c THIS PAGE **unclassified**	**SAR**	**4**	

Standard Form 298 (Rev. 8-98)
Prescribed by ANSI Std Z39-18

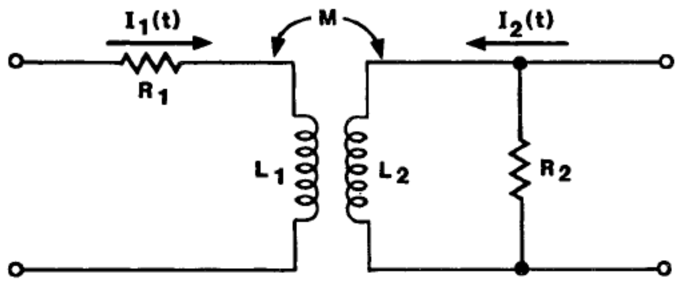

Figure 1. Idealized transformer

If $\alpha^2 > \omega_o^2$, then, the resulting time expressions for the currents are

$$I_1(t) = \frac{(\omega^2 - \alpha^2)\ M}{\omega R_1 R_2}\ e^{-\alpha t}\ \sinh\ \omega t$$

$$I_2(t) = \frac{1}{R_1}\Big[1 - e^{-\alpha t}\ \cosh\ \omega t$$

$$+ \frac{(\alpha^2 - \omega^2)L_2 - \alpha R_2\ \sinh\ \omega t}{\omega R_2}\Big]$$

The general expression for currents,

$$I_1(t) = \frac{1}{R_1}\Big[1 = \frac{\sigma T_1 T_2}{(T_1 + T_2)q}\Big[(\beta - \frac{R_1}{T_2})e^{-\alpha t}$$

$$- (\alpha - \frac{R_1}{T_2})e^{-\beta t}\Big]\Big]$$

$$I_2(t) = -\frac{M}{R_1 R_2} \cdot \frac{1}{(T_1 + T_2)q}\ (e^{-\alpha t} - e^{-\beta t})$$

Where,

$$\sigma = \sqrt{1 - \frac{M^2}{L_1 L_2}}\ ;\ T_1 = \frac{L_1}{R_1}\ ;\ T_2 = \frac{L_2}{R_1}$$

$$q = 1 - \frac{4\sigma T_1 T_2}{(T_1 + T_2)^2}\ ;\ \alpha = \frac{T_1 + T_2}{2\sigma T_1 T_2}\ (1 - q)\ ;$$

$$\beta = \frac{T_1 + T_2}{2\sigma T_1 T_2}\ (1 + q).$$

It is evident that the performance of the pulse transformer in terms of energy transfer and fidelity increases as $k = M/\sqrt{L_1 L_2}$ approaches unity, requiring tighter and tighter couplings between the primary and secondary. Reference 3 gives several methods in which this can be achieved. The secondary is to be, effectively, a single turn, split in several sections. The sections are parallel connected, each pairing with one turn in the primary and "compensating" it as well as possible. Different shapes for the cross-sectional area of the different turns would give different coefficients of coupling. In such situations in which the flux difference for the primary and secondary is very small, the regular formulae, based on idealized assumptions (infinite length, homogeneity, etc.) would produce inadmissible errors. For a good engineering design, flux plots for the real configuration were used. Three cases have been considered; parallel plates, parallel conductors, and coaxial conductors.

An axisymmetric finite element electromagnetic code has been used for aclculating the leakage inductance. The flux plots are given in Figures 2, 3, and 4, respectively. It was found that the coaxial construction is by far the most effective, and for this reason such a structure was chosen. Also, for the coaxial configuration the flux plot and the theoretical formula[3]

$$k = 1 - \frac{(\ln \frac{r_o}{r_i} + \frac{1}{4})}{k\pi\ N(\frac{R}{\ell})}$$

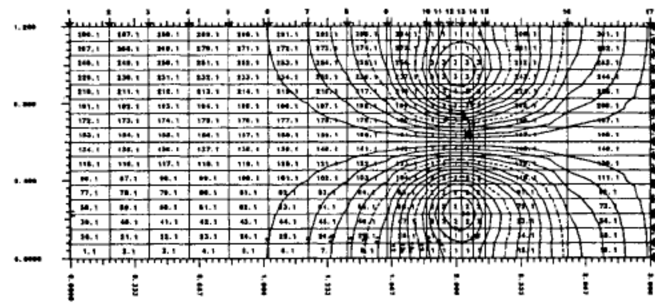

Figure 2. Flux plot: parallel conductors

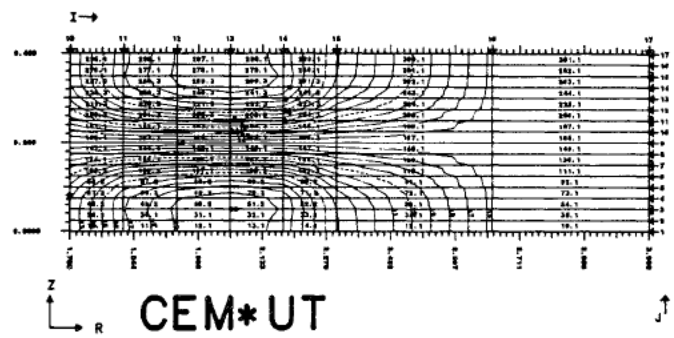

Figure 3. Flux plot: parallel plates

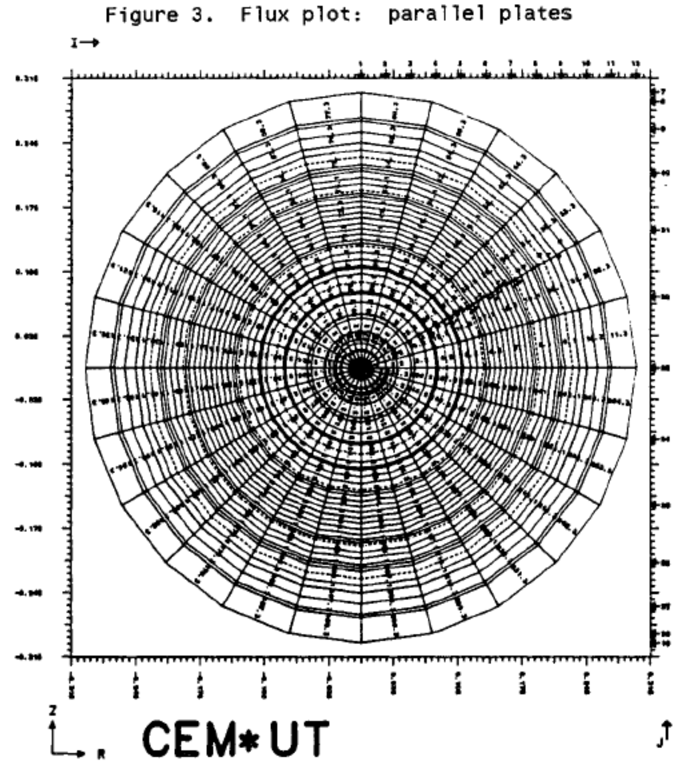

Figure 4. Flux plot: coaxial cable

where,

r_o = radius, outer conductor
r_i = radius, inner conductor
R = radius of turn
ℓ = length of the pulse transformer

have the best agreement.

The slight disagreement with measured data can be explained be the transient skin effect which reduces the equivalent inductances of both primary and secondary windings while increasing the resistance.

The forces are calculated using the magnetic pressure on the conductors:

$$p = \frac{1}{2\mu} [B^2(o,t) - B^2(x,t)]$$

In the case of rapid pulses and transient field diffusion the transient depth of penetration is taken into account. Once again the coaxial cable construction is advantageous with regard to forces in comparison with all other competing topologies. However, there is an "uncompensated" region in the location of the connection of the secondary conductors to the busbars. Even if the pulses are short, they still do not meet the requirements for dynamic containment where the time duration of the magnetic pressure pulse is short compared with the oscillating period of the container. However, we have extrapolated the criterion and the results were satisfactory.

Design and Fabrication

This transformer is shown schematically in Figure 5 and the major design parameters are presented in Table 1.

Table 1. Design parameters

Maximum input current	100 kA
Primary turns	4
Secondary turns	10 kA
Maximum output current	400 kA

A simplified model of the the test bed was used to predict the performance of the transformer where, L_c is the internal inductance of the store, R_p and R_s are the lumped resistances of the primary and secondary, respectively. L_L and R_L comprise the load and were assumed to be constant. V_o is the charge voltage on the store, C. The coupling coefficient, $k^2{}_c$ was in excess of 0.9. It was also assumed that the walls of the secondary were thick enough that the field did not diffuse through them in the discharge time.

Initial analyses showed that a smaller diameter primary cable could be used if the number of primary turns was increased. This led to the final configuration of a five turn primary consisting of 4/0, 15 kV jumper cable.

The secondary was chosen to be five pieces of 6.033-cm thick wall aluminum pipes bent into rings and connected in parallel. The dimensions of the secondary conductor were fixed by the required wall thickness and the ability of a shop to bend the pipe.

The performance of the pulse transformer consisting of these components was predicted using the model. The results are summarized in Table 2.

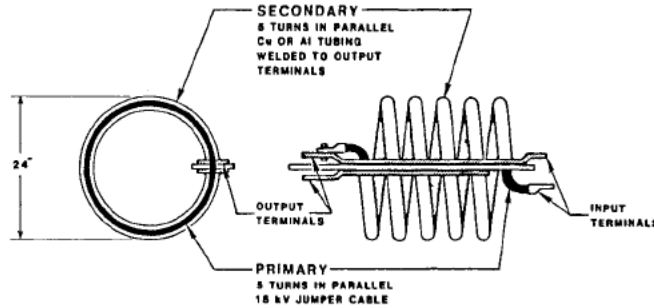

Figure 5. Pulse transformer

Table 2. Predicted Performance Characteristics

V_o =	8.50 kV
R =	6.64 mΩ
R =	6.40 μH
I_1 =	100 kA
I_2 =	440 kA

Time-to-peak 122 μs

The structure of the transformer was designed to withstand the peak loads encountered during discharge. The material used for the secondary, annealed 6061 aluminum, has a yield strength approximately 40 times the maximum stress on the inside walls of the tubes, so deformation of the secondary winding was not an important consideration. The peak pressure exerted on the output busbars, however, is considerably larger. The output of the transformer is 1.27-cm aluminum plate. The plates are restrained with 5-cm thick-wall steel box beams bolted together with a preload to minimize deflection. The peak force of repulsion on the output plates is 45 kN distributed over an area of 21 mm^2. A dynamic analysis showed that the deflection of the box beams should be less than 0.03 mm.

The transformer proved to be simple to fabricate, particularly in light of the fact that the coupling between the primary and the secondary was required to be high. The aluminum tubes were bent into 180 degrees turns and welded together to form the secondary helix. The method used to assemble the secondary was to first weld one half of the tubes to the common Figure 7. Welding at alignment plate busbar and the alignment plate. The polyethylene insulator was then installed into the common plate by aligning it over the openings, clamping it in place and forming it into shape by heating the area around the openings (fig. 6). The remaining half of the helix was then assembled and welded. The two halves were mated and welded at the alignment plate.

The primary conductor was pulled through the completed helix using methods common to conduit wiring. Electrical connection between the primary and secondary, and primary and input plate was accomplished using thick wall copper tube crimped onto the primary cable and clamped to the buswork. The assembly was completed with the installation of the retainer clamps along the length of the connection plates (fig. 7).

Performance

The only testing performed on the pulse transformer was to discharge the device into a short circuit. The energy stores used were a 180 μF capacitor bank at 1 to 4 kV and a 1,100 μF capacitor bank at 5 to 8 kV. The transformer exceeded the design goals by delivering 450 kA into a short circuited secondary at a capacitor charge voltage of 8 kV. Primary and secondary current traces are shown in Figure 9. The results of the test series are presented in Table 3.

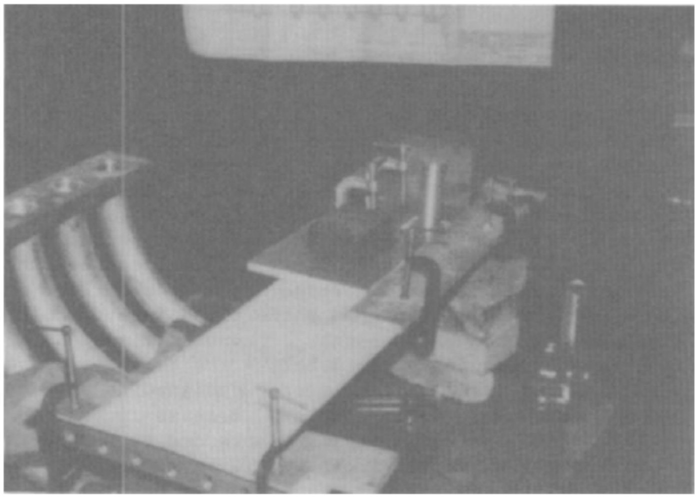

Figure 6. Polyethylene insulator installed into common plate

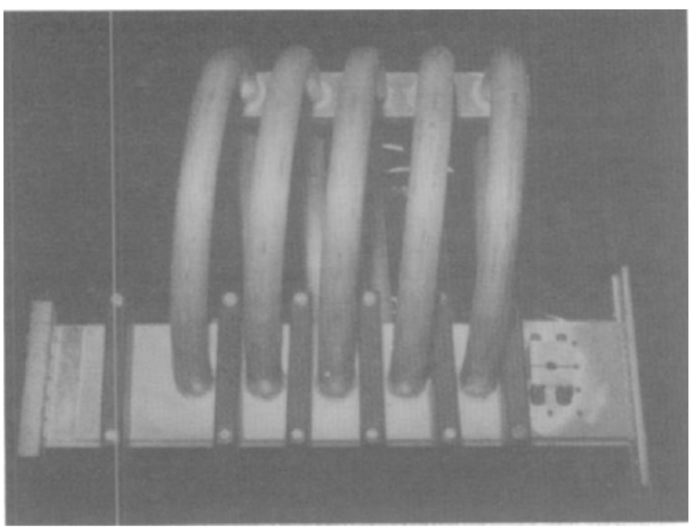

Figure 7. Completion of assembly

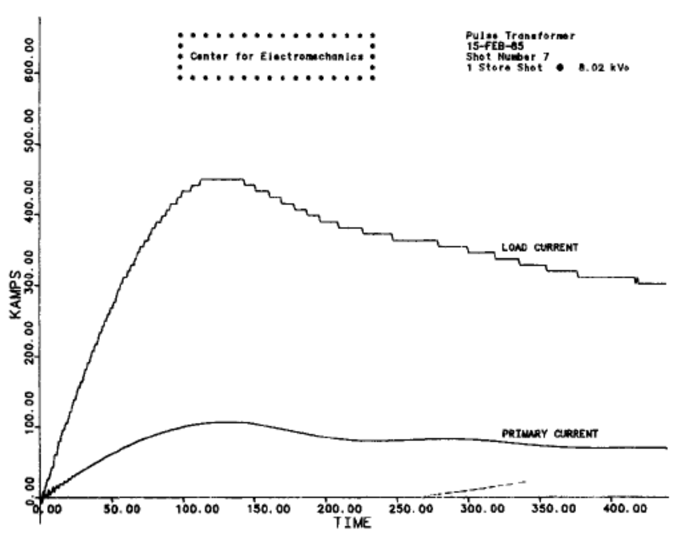

Figure 8. Discharge currents for the pulse transformer

Table 3. Summary of Test Results

V	C	Primary Current PK		Secondary Current PK		I_2/I_1
kV	µF	kA	µs	kA	µs	(peak)
1	180	5.5	54	24	50	4.4
2	180	11	53	49.5	51	4.5
4	180	23	53	101	51	4.4
5	1,100	54	132	230	105	4.2
6	1,100	80	121	350	118	4.4
7	1,100	92	125	400	119	4.3
8	1,100	110	125	450	110	4.1

While the output plates of the transformer were not instrumented for dynamic force measurement, the plates and the box beams were measured following each discharge with a micrometer. No permanent deformation was measured. A hairline crack developed in one of the welds on the primary cable clamps during the high energy discharge. This was from the solenoidal forces compressing the primary coil as a result of uncoupled flux. However, the weld should have been able to easily withstand the force, and the defect was traced to a faulty modification to the welded part.

Conclusion

The coaxial pulse transformer has been fabricated and tested. The performance of the device has demonstrated the high degree of coupling possible.

Variations on and modifications to the original geometry can improve the coupling, including reducing the air gap between the primary and secondary. A further improvement in the performance of the device could be realized by improving the topology and the material for the secondary.

Acknowledgements

The authors are indebted to the technical staff at CEM-UT for their assistance in the design and construction of the transformers. In addition, the authors acknowledge the assistance by J. Bennet in formulating a model for the device and by A. Zielinski, who tested the first laboratory model.

References

1. Ferrentino, G., "AGATE: On the Design of a Hypervelocity Railgun Launcher," proceedings of the 5th Pulsed Power Conference, 1985.
2. Vitkovitski I. M., et. al, "Homopolar Current Source for Mass Accelerators," proceedings of the 1980 Conference on Electromagnetic Guns and Launchers," p. 157.
3. Sadedin, D. R., "Geometry of a Pulse Transformer for Electromagnetic Launchers," proceedings of the Second Symposium on Electromagnetic Launch Technology, p. 381.
4. Kitagawa, S. and Hiranok, I., "Fast Power 'Crowbar' System Using a Current Transformer with Extremely Low Leakage Inductance," Rev. Sci. Instrum., Vol. 45, No. 7, July 1974, p. 962.
5. Driga, M. D., et. al, "Methods for Producing the Plasma Initiation Pulse in Ohmic Heating Circuits in Tokomak Power Reactors," Proceedings of the Seventh Symposium on Engineering Problems of Fusion Research, Vol. 1, p. 473.